

Risk Analysis for Landslides and Snow Avalanches

Example applications for snow avalanches

522051-1

23 December 1999

Client: NGI / Research Council of Norway

Contact person: -
Contract reference: SIP4 – 110681/420

For the Norwegian Geotechnical Institute

Project Manager: Frode Sandersen

Report prepared by:

Farrokh Nadim
Farrokh Nadim

Reviewed by:

Carl B Harbitz
Carl Harbitz



Summary

Prediction of snow avalanche occurrence and its run-out distance inherently involves many uncertainties. The main reason for the large uncertainties is that the mechanical behaviour of snow is extremely complicated, and other external factors that affect the problem, such the climate, wind direction, amount of snowfall, loading rate, etc. are all more-or-less random processes. The aim of the work described in this report is to demonstrate potential applications of probabilistic analysis to problems related to snow avalanches.

Two problems are looked into. The first problem is evaluating the probability of a slab avalanche. A mechanical model based on traditional geotechnical approach to slope stability was adopted. To account for the uncertainties in the input parameters, the stability model was coupled to reliability analysis software. In addition to the failure probability, the probabilistic analyses provide the most likely combination of parameters at failure and the sensitivity factors that quantify the contribution of each random variable to the total uncertainty.

The second problem considered is related to the development of hazard maps for snow avalanche. Current practice is to use a statistical model for run-out distance in areas where topography and climate are favourable for avalanche activity. The procedure may be conservative because it basically assumes that in the area of interest, avalanche activity occurs every year. The actual annual probability of snow avalanche occurrence at a given area is ignored because it is difficult to estimate this probability from physical models. A procedure is outlined in the report to use historical observations and Bayesian updating to estimate the annual probability of snow avalanche occurrence. The procedure is demonstrated through an example application.

Recommendations for further studies are made at the end of the report.



Contents

1	INTRODUCTION.....	4
2	PROBABILISTIC ANALYSIS OF SNOW-SLAB AVALANCHE.....	4
	2.1 The “standard” snow-slab avalanche.....	4
	2.2 Probabilistic model for snow-slab avalanche	6
	2.3 Example calculation results	9
	2.4 Conclusions	13
3	AVALANCHE HAZARD MAPPING	16
4	RECOMMENDATIONS FOR FURTHER STUDIES.....	21
5	REFERENCES.....	21

Review and reference document



1 INTRODUCTION

Prediction of snow avalanche occurrence and its run-out distance inherently involves many uncertainties. The main reason for the large uncertainties is that the mechanical behaviour of snow is extremely complicated, and other external factors that affect the problem, such the climate, wind direction, amount of snowfall, loading rate, etc. are all more-or-less random processes.

To make rational decisions under large uncertainty, one should properly account for them. This report presents two example applications of probabilistic analyses for the snow avalanche problem. The demonstration examples are highly simplified and are meant to highlight typical application areas.

2 PROBABILISTIC ANALYSIS OF SNOW-SLAB AVALANCHE

Field observations and measurements show that the physical mechanism governing the release of a slab avalanche can differ greatly depending on the character of the deformation in the weak layer or interface beneath the slab where the slide initiates (McClung, 1986). The initiation of a slab avalanche is a multi-phase and progressive fracture process. Referring to Fig.1, Lackinger (1989) describes the following stages of a snow-slab avalanche fracture:

- Shear fracture along the shear interface, which is more-or-less parallel to the surface.
- Tensile fracture at the crown of the snow-slab avalanche.
- Flank fracture at the sides of the slab.
- Compressive fracture at the staunch wall.

The common practice is to investigate the slab stability solely with respect to shear fracture in the shear interface, disregarding the boundary conditions along the entire snow-slab area, as well as the fracture's progressive character. A stability factor (safety factor in the geotechnical sense), "s" is defined as the ratio of the shear strength along the potential failure plane and the driving shear stress parallel to the slope surface. The stability factor method has often proved to be unsatisfactory in practice (Lackinger, 1989). Therefore, in the mechanical model described below, the total potential avalanche is considered.

2.1 The "standard" snow-slab avalanche

The following forces act on the "standard avalanche" shown on Fig. 2.1: T is the driving component of the total weight W , F_T is the tension force at the crown, F_C is the compression force at the staunch wall, F_F is the flank force and F_S is the shear force along the shear surface. These forces can be estimated from the following equations:

A safety factor may be defined as the ratio of the total resisting forces in the down-slope direction to the driving shear force:

$$SF = (F_S + F_T + F_C + F_F) / T \quad (2.7)$$

According to Perla (1980), the “standard avalanche” is characterised by the following values: $\rho = 220 \text{ kg/m}^3$, $B = 50 \text{ m}$, $L = 50 \text{ m}$, $D = 0.7 \text{ m}$ and $\psi = 38^\circ$. Lackinger (1989) performed a parametric study of the “standard” snow-slab avalanche using the following ranges of strengths:

Parameter	Minimum strength (kPa)	Maximum strength (kPa)
σ_t	3	15
c	2.5	10
τ_s	0.5	5

With the minimum values of all strength parameters, the evaluated safety factor is only 0.72, whereas using the maximum values results in a safety factor of 6.09.

The range of safety factor clearly shows the practical problem one is faced with in a deterministic approach. When there is large uncertainty in the actual value of important parameters, a probabilistic approach capable of accounting for the uncertainties is called for. A probabilistic model for “standard” snow-slab avalanche is described in the following section.

2.2 Probabilistic model for snow-slab avalanche

The deterministic model described in previous section may be used in conjunction with the first-order reliability method (FORM) in order to perform probabilistic snow-slab stability analysis.

The FORM approximation requires the definition of a performance function $g(X)$, such that $g(X) \geq 0$ means that the slope is stable and $g(X) < 0$ means that the slab avalanche will occur. X is a vector of basic random variables including snow strength properties, external load effects, geometry parameters and modelling uncertainty.

If the joint probability density function for all random variables, $F_x(X)$ is known, then the probability of failure P_f is given by

$$P_f = \int_L F_x(X) dX \quad (2.8)$$

where L is the domain of X where $g(X) < 0$. In general the above integral cannot be solved analytically, and an approximation is obtained by the FORM approach. In this approach, the general case is approximated to an ideal situation where X is a vector of independent Gaussian variables with zero mean



and unit standard deviation, and where $g(X)$ is a linear function. The probability of failure P_f is then:

$$P_f = P(g(X) < 0) = P\left(\sum_{i=1}^n \alpha_i X_i + \beta < 0\right) = \Phi(-\beta) \quad (2.9)$$

where $P(\dots)$ reads “the probability that”, α_i is the direction cosine of random variable X_i , β is the distance between the origin and the hyperplane $g(X) = 0$, n is the number of basic random variables X , and Φ is the standard normal distribution function. The vector of the direction cosines of the random variables (α_i) is called the vector of sensitivity factors, and the distance β is called the reliability index.

The higher the value of reliability index β , the smaller the probability of failure. The square of the direction cosines or sensitivity factors (α_i^2), which sum is equal to unity, quantifies in a relative manner the contribution of the uncertainty in each random variable X_i to the total uncertainty.

The FORM approximation is done in two steps:

1. The vector of basic random variables X is transformed into a vector U of independent Gaussian variables with zero mean and unit standard deviation using Rosenblatt's (1952) transformation.
2. The (transformed) limit state function is linearised at the point of maximum probability density. This is the most likely “failure” point and is referred to as the “design point”. The design point is found by optimisation techniques.

The design point u^* , reliability index β , sensitivity vector $\bar{\alpha}$, and the FORM approximation are shown schematically on Fig. 2.2 for two random variables.

The statistical subroutine package STRUREL developed by RCP GmbH (1999) was used for the FORM approximation in the probabilistic snow-slab stability calculations.

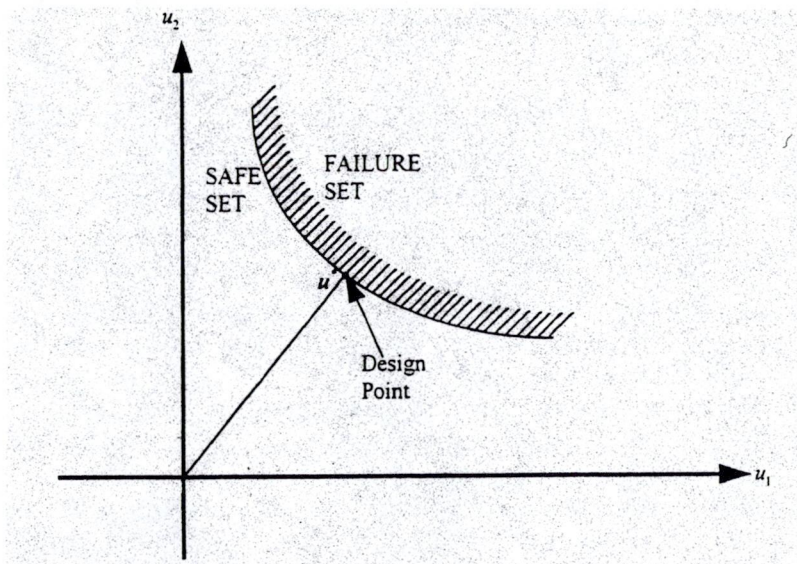
The performance function for the snow-slab stability was defined as:

$$g = SF - 1 \quad (2.10)$$

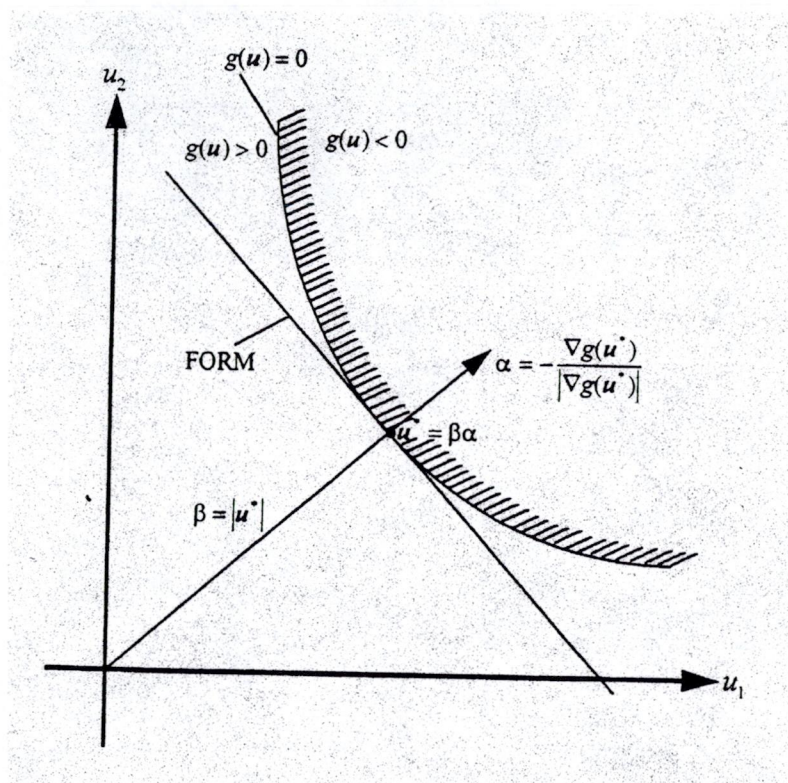
where SF is the safety factor defined by Eq. 2.7.

One way of accounting for modelling uncertainty is to introduce a random variable ε to describe the uncertainty introduced by the mathematical idealisation of the problem. In this situation the performance function reads

$$g = SF \cdot \varepsilon - 1 \quad (2.11)$$



(a) Design point



(b) Linearisation of limit state function in u-space

Fig. 2.2 The FORM approximation for two variables in the transformed, standardised normal space (u-space).



For an accurate model, ϵ is typically assumed to have a normal distribution with mean value of 1.0 and standard deviation of 5 – 10%. However, in some situations standard deviation of 15, 20, or even 30% is appropriate (Lacasse and Nadim, 1996). Model uncertainty is best evaluated from well-designed model tests and back-calculations of failures.

The model uncertainty was neglected in the example calculations, because including it would have overshadowed all other uncertainties.

2.3 Example calculation results

The “standard” slab avalanche was used in the example calculations to demonstrate that reliability methods are basically powerful tools for systematic parametric studies.

Nine basic random variables were defined with the probability distributions given in Table 2.1. The mean values and standard deviations were chosen such that most parameters fall within the range considered in the parametric studies by Lackinger (1989). A correlation coefficient of $\rho(c, \sigma_t) = 0.8$ was assumed between the cohesive and tensile strengths of snow (see Ang and Tang, 1975, for definition of correlation coefficient).

Table 2.1 Probability distribution of basic random variables in the standard avalanche model.

Random variable	Distribution	Mean	Standard deviation	Range considered by Lackinger (1989)
Thickness (or height) of slab, D	Lognormal	0.7 m	0.1 m	0.4 – 1.5 m
Slope angle, ψ	Lognormal	38°	3°	38°
Cohesive strength of snow, c	Lognormal	6 kPa	1.5 kPa	2.5 – 10 kPa
Tensile strength of snow, σ_t	Lognormal	9 kPa	2.4 kPa	3 – 15 kPa
Shear strength of sliding plane, τ_s^*	Lognormal	1.046 kPa	0.321 kPa	0.5 – 5 kPa
Width of slide, W	Lognormal	50 m	25 m	10 – 110 m
Length of slide, L	Lognormal	50 m	25 m	10 – 110 m
Density of snow, ρ	Normal	220 kg/m ³	20 kg/m ³	220 kg/m ³
External load, W_{ex}^{**}	Lognormal	10 kN	2 kN	0

* Expected value = 1 kPa, coefficient of variation = 30%

** $W_{ex} = 0$ in the standard slab avalanche model

STRUREL allows the user to perform parametric studies for one or more random variables where the mean and standard deviation of that variable are increased or decreased by the same factor and the effects on the results are evaluated. This option was used for the slab thickness, for which a range corresponding to 0.5 to 1.5 times the base case value (i.e. average thickness of $0.5 \cdot 0.7 = 0.35$ m to $1.5 \cdot 0.7 = 1.05$ m) was considered in the analyses. With the base case values, a failure probability of $P_f = 0.023$ and corresponding reliability index of $\beta = 1.99$ were computed. Figure 2.3 shows the computed sensitivity factors (α_i in Eq. 2.7) and their squares. It can be seen that the uncertainty in the shear resistance of the sliding plane (weakness plane) is the most important contributor to the total uncertainty. This is followed by the length of the avalanche, the snow density, the cohesive and tensile strengths of snow, the slope angle, and the width of the avalanche, which contribute more-or-less equally to the total uncertainty. The uncertainties in the external load and the slab avalanche thickness do not contribute much to the total uncertainty.

Figure 2.4 shows the most likely combination of the random variables leading to failure (i.e. the values of random variables at the “design point”). The values are expressed as partial safety factors to be applied to “characteristic” values, which in this example are assumed to be identical to the mean values.

Figure 2.5 shows the variation of failure probability as function of the thickness of slab avalanche. The horizontal axis is the factor that is applied to the mean and standard deviation of slab thickness ($PAR1 = 1.0$ corresponds to mean slab thickness of 0.7 m). Figures 2.6 and 2.7 respectively show the variation of sensitivity factors and partial safety factors versus the mean slab thickness.

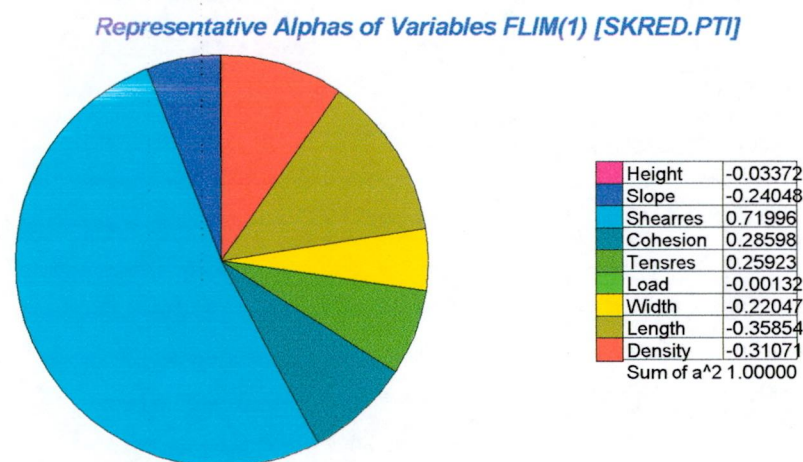


Figure 2.3 Sensitivity factors for basic random variables. Base Case.

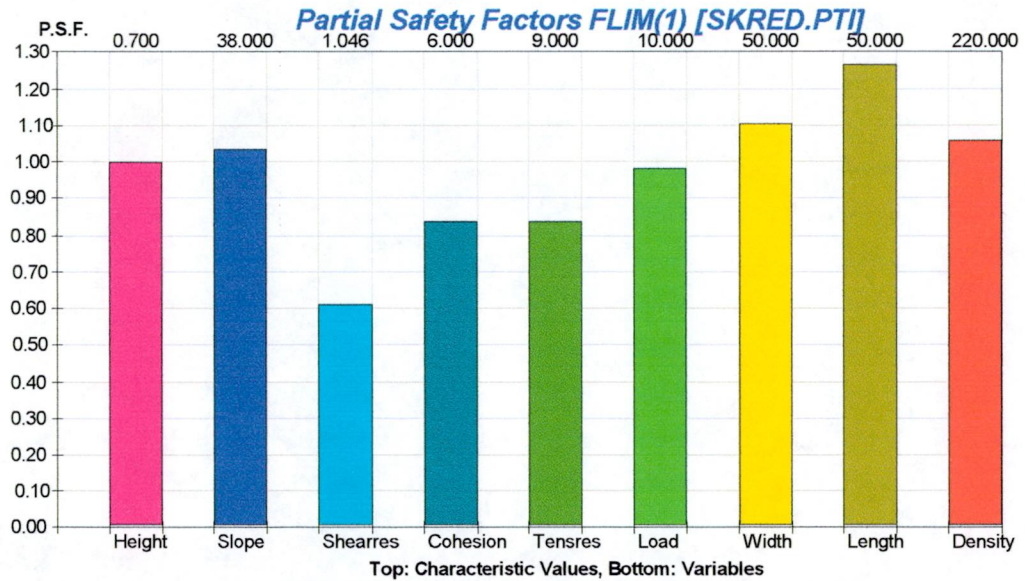


Figure 2.4 Partial safety factors at most-likely failure point. Mean values are used as characteristic values. Base case.

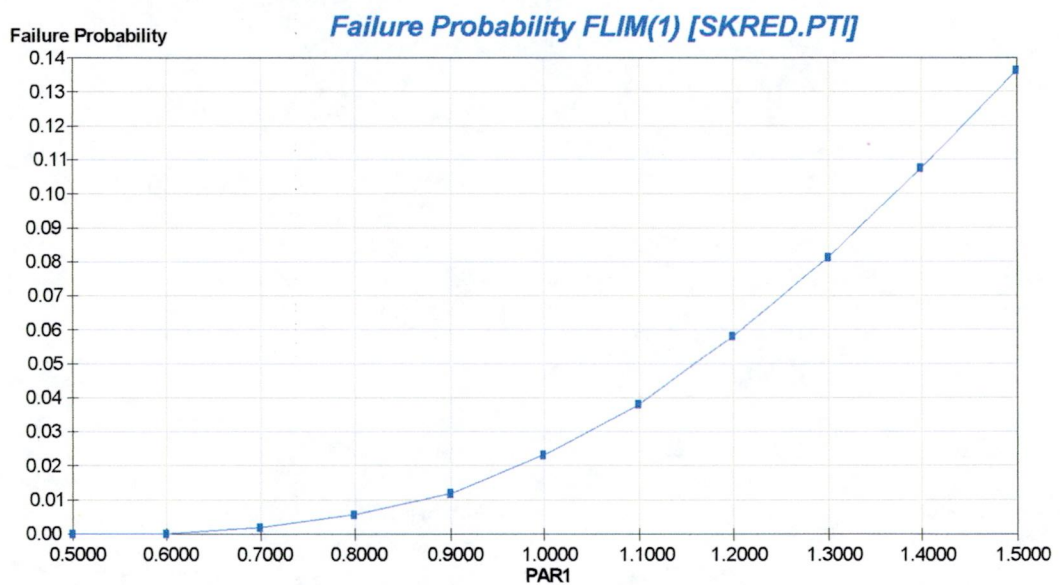


Figure 2.5 Variation of failure probability versus the thickness of slab avalanche. PAR1 = 1.0 corresponds to mean slab thickness of 0.7 m. Base Case.

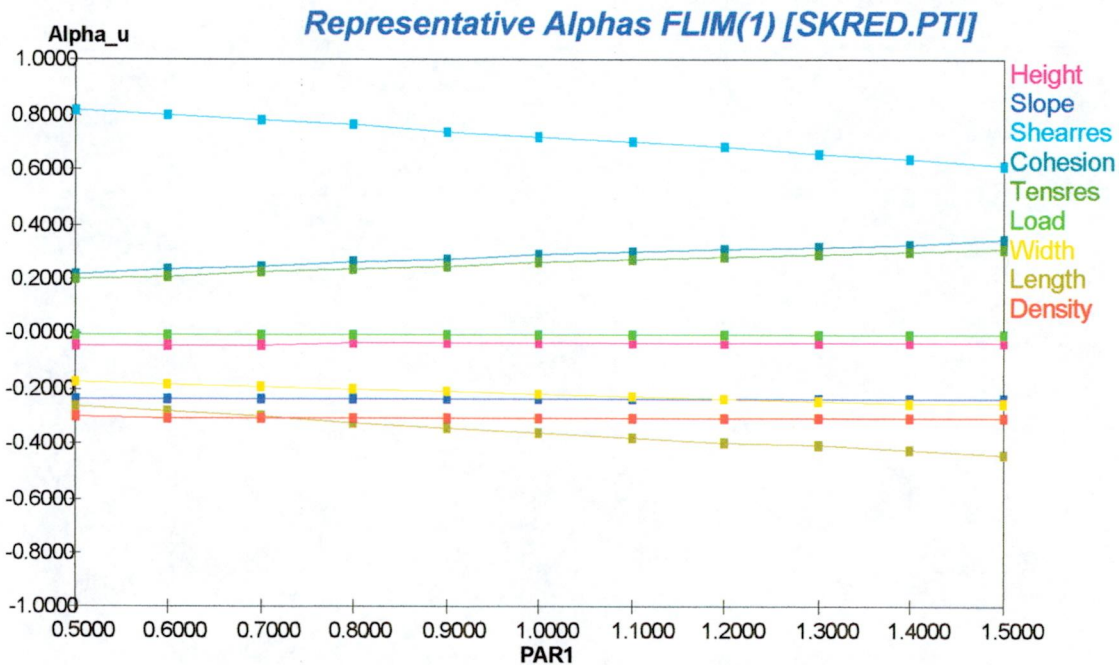


Fig. 2.6 Variation of sensitivity factors versus the mean slab thickness. PAR1 = 1.0 corresponds to mean slab thickness of 0.7 m. Base Case.

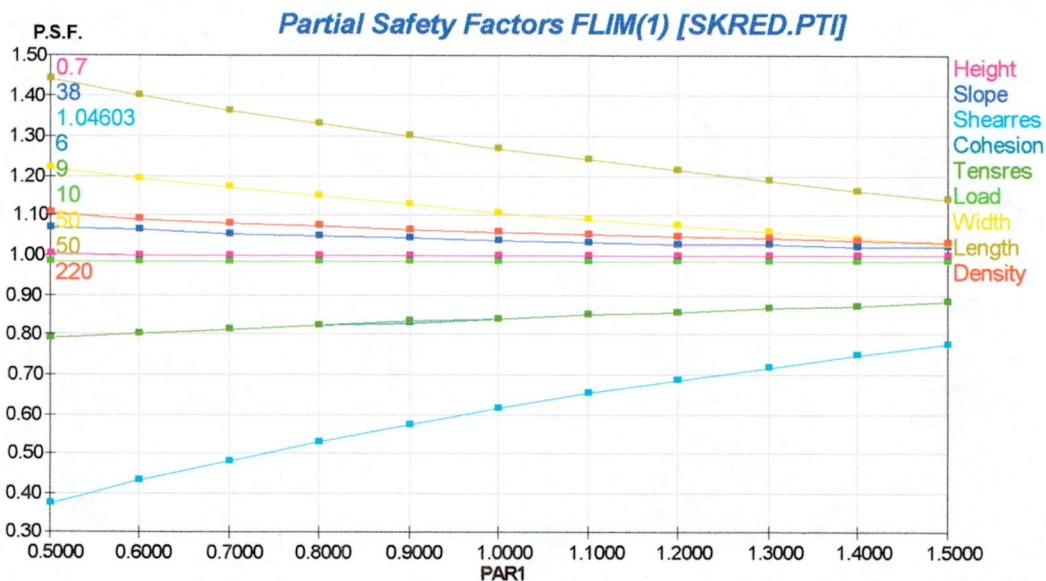


Fig. 2.7 Variation of partial safety factors versus the mean slab thickness. PAR1 = 1.0 corresponds to mean slab thickness of 0.7 m. Base Case.



According to McClung (1996), there is a scale effect on the average shear resistance of the weakness plane such that larger areas tend to have a lower shear resistance. To model this effect qualitatively, the Base Case example was re-analysed assuming a negative correlation between the average shear resistance and width and length of the slide, i.e. $\rho(\tau_s, W) = -0.5$ and $\rho(\tau_s, L) = -0.5$. All other assumptions regarding the probability distributions and correlation coefficients were kept unchanged. In this situation, a failure probability of $P_f = 0.057$ and corresponding reliability index of $\beta = 1.58$ were obtained for the standard avalanche. Figures 2.8 through 2.12 show the results obtained for this case.

It can be seen that the scale effect significantly increases the probability of failure (more than a factor of 2 for $D = 0.7$ m) and the uncertainties in shear resistance of the plane of weakness and surface dimensions of the slide completely dominate the total uncertainty. Furthermore, the surface area of the slide is likely to be greater (compare the partial safety factors for width and length in Figs. 2.4 and 2.9) because a larger surface will tend to have a lower shear resistance. Figures 2.4 and 2.9 show that the most likely scenario for occurrence of the slab avalanche is that the shear strength of the plane of weakness is about 0.6 kPa, while simultaneously there are small perturbations in strength and density of the snow with respect to the estimated mean (or characteristic) values.

2.4 Conclusions

The example application presented in this section demonstrates that the first-order reliability method is a powerful tool for performing systematic parametric studies. It provides the engineer with a rational framework for decision making when there is a large uncertainty in the input parameters, and it identifies the relative contribution of the input variables to the overall uncertainty. This information helps the engineer to focus on reducing the uncertainty in a few important parameters in order to achieve a significant reduction in the overall uncertainty.

Representative Alphas of Variables FLIM(1) [SKRED.PTI]

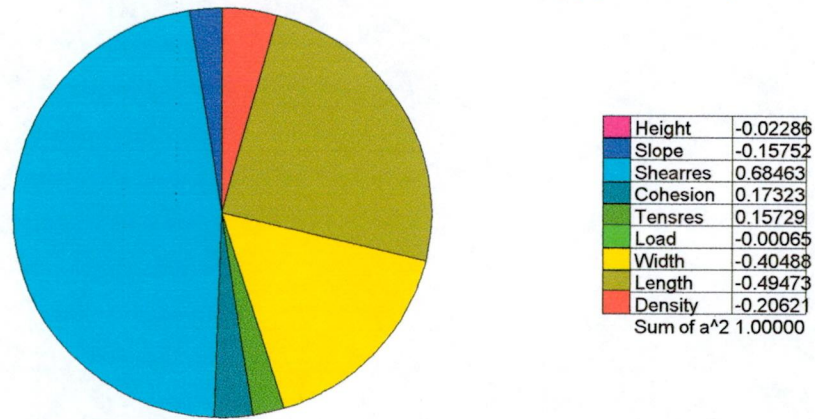


Figure 2.8 Sensitivity factors for basic random variables. Negative correlation between shear resistance and dimensions of avalanche.

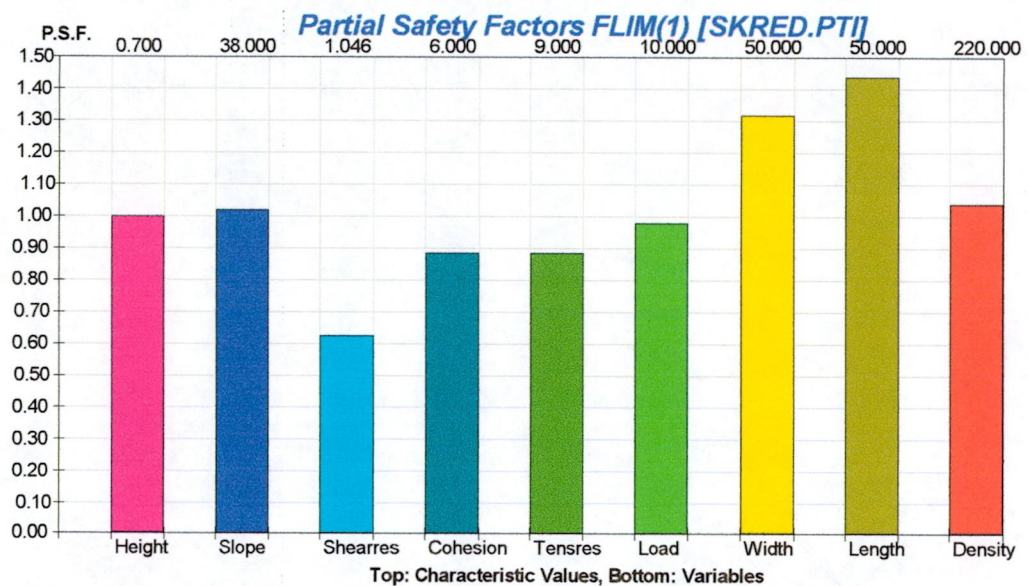


Figure 2.9 Partial safety factors at most-likely failure point. Mean values are used as characteristic values. Negative correlation between shear resistance and dimensions of avalanche.

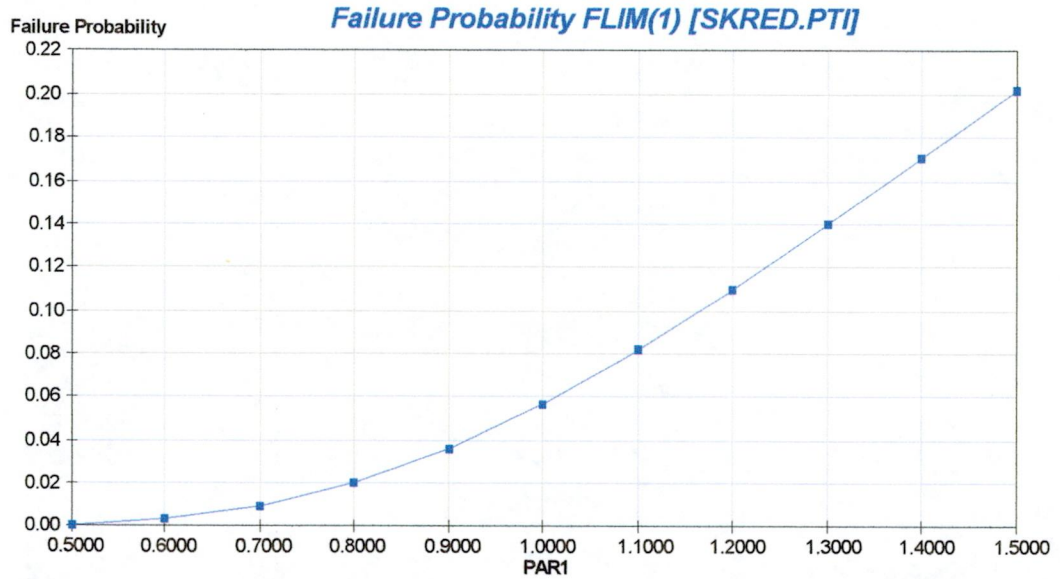


Figure 2.10 Variation of failure probability versus the thickness of slab avalanche. PAR1 = 1.0 corresponds to mean slab thickness of 0.7 m. Negative correlation between shear resistance and dimensions of avalanche.

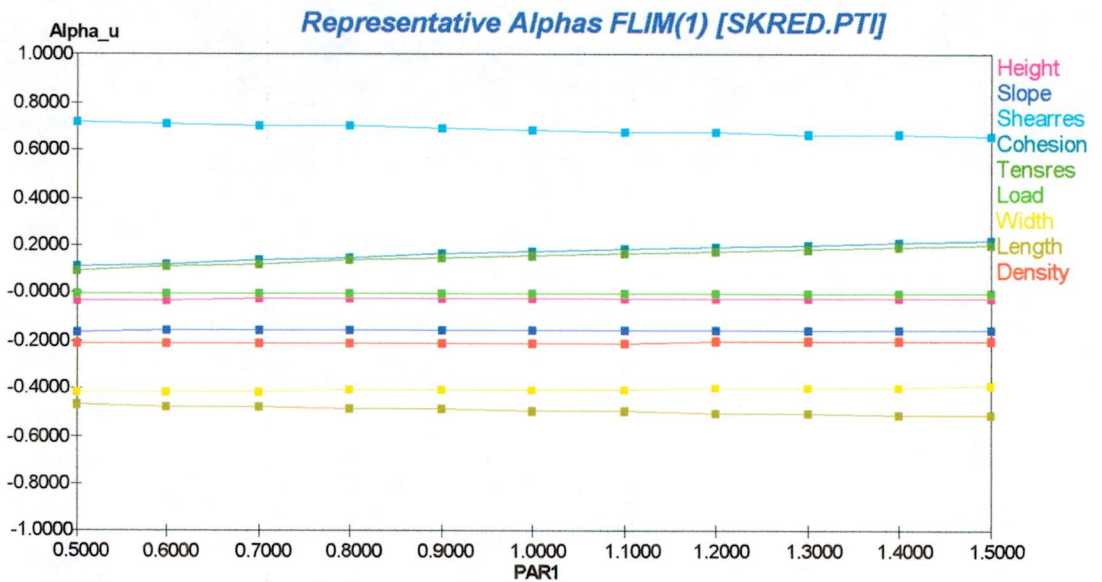


Fig. 2.11 Variation of sensitivity factors versus the mean slab thickness. PAR1 = 1.0 corresponds to mean slab thickness of 0.7 m. Negative correlation between shear resistance and dimensions of avalanche.

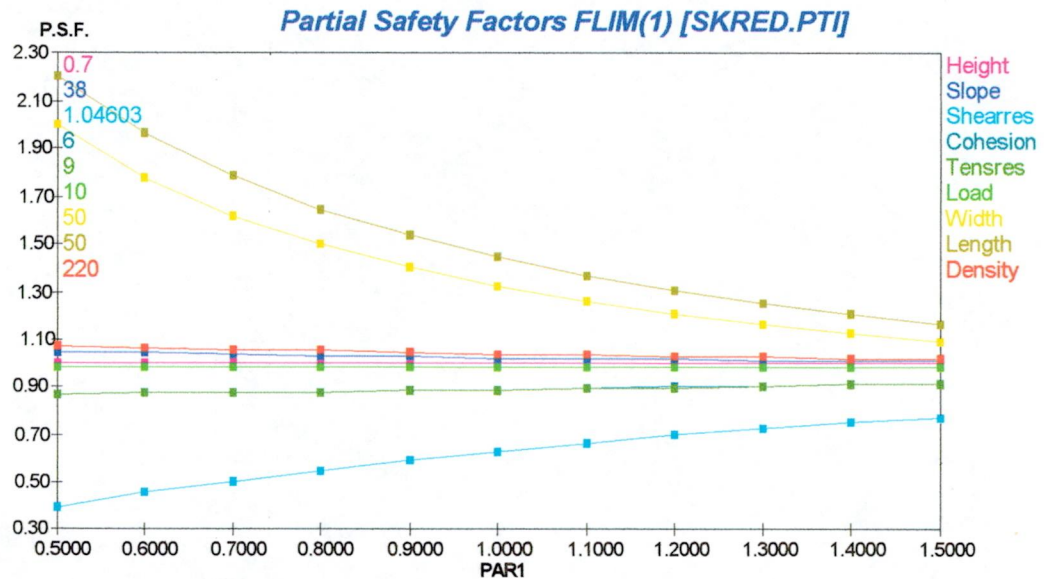


Fig. 2.12 Variation of partial safety factors versus the mean slab thickness. PAR1 = 1.0 corresponds to mean slab thickness of 0.7 m. Negative correlation between shear resistance and dimensions of avalanche.

3 AVALANCHE HAZARD MAPPING

The “safe” areas in the snow-avalanche prone regions of Norway are defined as areas where the annual probability of a house being hit by an avalanche is less than 10^{-3} (Norwegian Building Regulations). In practice, the demarcation line between the safe and unsafe areas is often established using the so-called α/β model (NGI, 1996).

The statistical α/β -model developed at NGI predicts the extreme run-out distance for a snow-avalanche solely as a function of topography. The run-out distance equations are found by regression analysis, correlating the longest registered run-out distance from 206 avalanche paths to a selection of topographic parameters. The parameters that have proved to be most significant are presented in Table 3.1 (see also Fig. 3.1).

The β -angle is empirically found to be the best characterisation of the track inclination, and the regression analysis revealed that the β -angle is also the most important topographic parameter. In fact, in general it would appear that β is the only statistically significant terrain parameter. A β -point is accepted only if it is inside the section of the profile where the angle between the tangent of the best-fit parabola and the horizontal plane is between 5° and 15° .

Table 3.1 Topographic parameters governing maximum run-out distance

Parameter	Description
β (deg.)	Average inclination of avalanche path between starting point and point of 10° inclination along terrain profile.
θ (deg.)	Inclination of top 100 vertical metres of starting zone.
H (m)	Total height difference between starting point and lowest point of best-fit parabola $y = c_2x^2 + c_1x + c_0$, where c_0 , c_1 , and c_2 are constants.
y'' (m^{-1})	$y'' = 2c_2$, related to curvature of avalanche path.

The inclination θ of the top 100 vertical metres of starting zone indirectly governs the rupture height, and thereby the slide thickness, which is greater in gentle slopes than in steep slopes. Hence smaller values of θ give longer run-out distances or smaller average inclination of the total avalanche path, α .

Smaller values of the product Hy'' mean smaller values of β . This results in theoretically smaller values of α , because the avalanches run with smaller velocity, and the velocity-dependent frictional transformation of potential energy into heat is reduced. Hence, the avalanches have an apparently lower coefficient of friction.

The topography, the width and the degree of lateral confinement in the starting zone, as well as the extreme drifting snow transport into the starting zone, have little influence upon the run-out distance. As opposed to what was presumed, no tendency was found that an avalanche with a wide rupture zone, which is channelled into a narrow track, has a longer reach than an avalanche following an unconfined path.

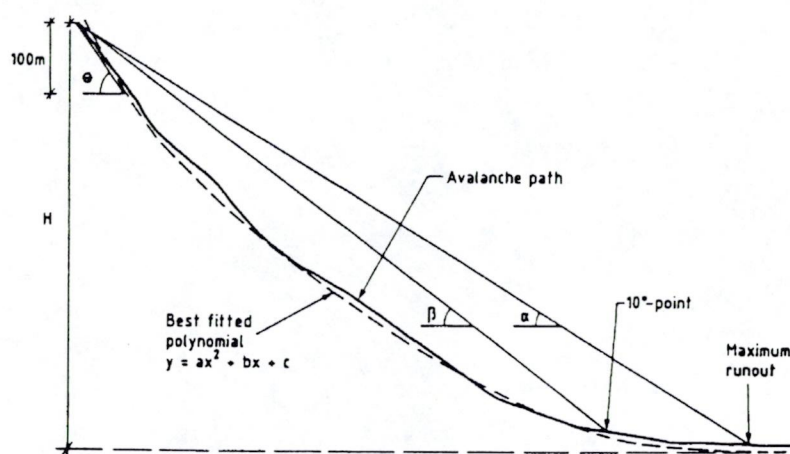


Figure 3.1 Topographic parameters describing terrain profile.

The model is most appropriate for travel distance analysis along longitudinally concave profiles. The calculated run-out distances are those that might be expected under snow conditions favouring the longest run-out distances.

The assumption of small variations in the physical snow parameters giving the longest run-out distance is only valid within one climatic region.

The avalanche database of NGI is constantly extended, and presently contains 230 events. The usual form of the α/β -model is that of a simple linear regression relation: $\alpha = m\beta + c$, where m and c are regression parameters. For the Norwegian data set, the values of m and c are respectively 0.96 and -1.4, and the standard deviation and correlation coefficient are respectively 2.3° and 0.92. Therefore, the predictive equation for maximum run-out distance reads:

$$\alpha = 0.96 \cdot \beta - 1.4^\circ + E \quad (3.1)$$

where $E = N(0, 2.3^\circ)$, i.e. a normally distributed random variable with mean of zero and standard deviation of 2.3° .

For some situations, the contour line defining the annual probability of less than 10^{-3} of being affected by an avalanche would correspond to α being about 3 standard deviations less than its mean value, i.e. $\alpha = 0.96 \cdot \beta - 1.4^\circ - 3 \cdot 2.3^\circ = 0.96 \cdot \beta - 8.3^\circ$. This is obviously a conservative approach that is not applicable to all situations. In practice, depending on the local climatic conditions, the snow avalanche expert estimates the 10^{-3} annual probability contour line based on expert judgement.

The reason the procedure above is conservative is that it basically assumes that in the area of interest, avalanche activity occurs every year. The “actual” annual probability is the probability computed from Eq. 3.1 times the annual probability of snow avalanche occurrence at a given area. It is very difficult to quantify the latter probability on the basis of physical models. In some areas where climatic conditions and topography are favourable for avalanche activity, local wind conditions may prevent the accumulation of snow and an avalanche would rarely occur. However, using a Bayesian approach (Ang and Tang, 1975) historical observations at a particular location could be used to estimate the probability of avalanche occurrence. In the Bayesian approach one updates the probability distribution function of a variable based on outcomes of experiments or observations. The updated or “posterior” probability distribution function is equal to a normalising constant times the product of the “prior” distribution function and the “likelihood function” implied by the observations.

Consider an area where climatic conditions and topography are favourable for avalanche activity. Without any recorded observations, the annual probability

of avalanche release could be anywhere between zero and one (see Fig. 3.2). In the Bayesian approach, this is known as a “diffuse prior” problem. If after “n” years of observation avalanche activity is observed in “r” years, it can be shown by the Bayesian approach the (posterior) annual probability of avalanche occurrence is (Ang and Tang, 1975):

$$f(P_{\text{avalanche}}) = K \cdot \frac{n!}{(n-r)!r!} P_{\text{avalanche}}^r (1 - P_{\text{avalanche}})^{n-r}, \quad 0 \leq P_{\text{avalanche}} \leq 1 \quad (3.2)$$

where K is a normalising factor. The expected value of $P_{\text{avalanche}}$ is:

$$E(P_{\text{avalanche}}) = \frac{r+1}{n+2} \quad (3.3)$$

which for large values of r and n approaches the statistical estimate of r/n.

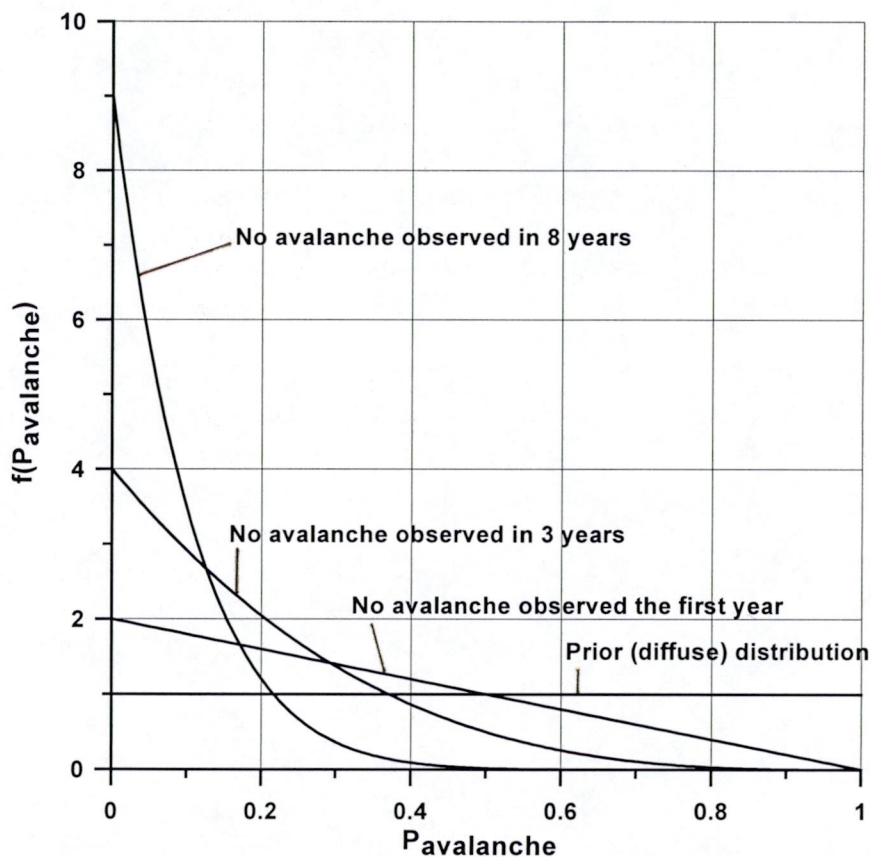


Figure 3.2 Probability distribution for annual avalanche occurrence after 0, 1, 3, and 8 years of observation of no avalanche.



If after “n” years of observation, no avalanche has yet taken place, then Eq. (3.2) reads:

$$f(P_{\text{avalanche}}) = (n+1)(1-P_{\text{avalanche}})^n, \quad 0 \leq P_{\text{avalanche}} \leq 1 \quad (3.4)$$

Figure 3.2 shows the probability distribution defined by Eq. 3.4 for $n = 0, 1, 3,$ and 8 years.

As an example application, we consider a location in Norway where the climate and topography are favourable for avalanche activity and the α/β run-out distance model described by Fig. 3.1 and Eq. 3.1 is valid. However, in the last 200 years that this area has been inhabited, there has been no record of any snow avalanche occurrence. The lack of snow avalanche activity in the area is probably due to the local wind conditions. Now, the local authorities wish to define the demarcation line between the areas deemed safe and the areas susceptible to avalanche (i.e. the line defining the annual probability of 10^{-3} of being hit by an avalanche). Using the historical evidence, the probability distribution for annual avalanche occurrence can be estimated from Eq. 3.4 with $n = 200$:

$$f(P_{\text{avalanche}}) = 201(1-P_{\text{avalanche}})^{200}, \quad 0 \leq P_{\text{avalanche}} \leq 1 \quad (3.5)$$

The probability that $P_{\text{avalanche}}$ is less than a specified threshold “X” is:

$$P[P_{\text{avalanche}} \leq X] = \int_0^X f(P_{\text{avalanche}}) dP_{\text{avalanche}} = 1 - (1-X)^{201}, \quad 0 \leq X \leq 1 \quad (3.6)$$

Using Eq. 3.6, the probability of annual avalanche occurrence being less than 10^{-3} is:

$$P[P_{\text{avalanche}} \leq 0.001] = 1 - (1 - 0.001)^{201} = 0.182$$

This means that there is an 18% probability that all areas are “safe” regardless of their location along the slope.

The median for annual occurrence of snow avalanche is:

$$1 - (1 - X)^{201} = 0.5 \Rightarrow X = 0.0034$$

The appropriate exceedance probability to use for the α/β model would be the target annual exceedance probability (10^{-3}) divided by the annual occurrence of snow avalanche. Therefore the median demarcation contour for the safe areas corresponds to $0.001/0.0034 = 0.294$ exceedance probability, which is the mean plus 0.52 times the standard deviation assuming normal distribution, i.e. α from Eq. 3.1 is equal to $0.96 \cdot \beta - 1.4^\circ - 0.52 \cdot 2.3^\circ = 0.96 \cdot \beta - 2.6^\circ$. Likewise, the



90% or any other confidence interval for the demarcation contour line may be computed:

$$\begin{aligned}
 1 - (1 - X)^{201} &= 0.9 \Rightarrow X = 0.0114 \\
 0.001/0.0114 &= 0.088 \Rightarrow \text{Mean} + 1.36 \text{ times standard deviation} \\
 \Rightarrow \alpha &= 0.96 \cdot \beta - 1.4^\circ - 1.36 \cdot 2.3^\circ = 0.96 \cdot \beta - 4.5^\circ \text{ (90\% confidence)}
 \end{aligned}$$

The best estimate of annual probability of avalanche occurrence is $E[P_{\text{avalanche}}] = 1/202$ (see Eq. 3.3), which following the procedure above leads to the best estimate demarcation contour corresponding to mean plus 0.84 times the standard deviation, i.e. α from Eq. 3.1 is equal to $0.96 \cdot \beta - 1.4^\circ - 0.84 \cdot 2.3^\circ = 0.96 \cdot \beta - 3.3^\circ$.

Note that in this example application, the statistical uncertainty associated with Eq. 3.1 was neglected in the evaluation of confidence intervals.

4 RECOMMENDATIONS FOR FURTHER STUDIES

Possible topics for further work on application of probabilistic analysis methods to snow avalanche problems are listed below.

- Implementation of probabilistic stability analysis for models that account for the dependence of the snow shear strength on the rate of deformation.
- Implementation of probabilistic stability analysis for models that account for progressive shear failure due to local stress concentration and fracture propagation on the weakness plane (unzipping mode of failure).
- Include the statistical uncertainty associated with Eq. 3.1 in the evaluation of confidence intervals and test the sensitivity of the results for other distributions of the angle α (there is some evidence that at a given location, a Gumbel distribution may be more appropriate).
- Use a physical model for snow avalanche occurrence to estimate the prior distribution (rather than the diffuse prior distribution assumed in the example problem).

5 REFERENCES

Ang, A. H-S., and W. Tang (1984)
Probability Concepts in Engineering Planning and Design.
John Wiley and Sons, New York.

Lacasse, S., and F. Nadim (1996)
Uncertainty in characterising soil properties.
Plenary paper, ASCE Conference Uncertainty '96, Madison, Wisconsin, 1-3 August.



Lackinger, B. (1989)

Supporting forces and stability of snow-slab avalanches: A parameter study.

Annals of Glaciology 13, pp. 140 – 145.

McClung, D.M. (1986)

Mechanics of snow slab failure from a geotechnical perspective.

Proceedings of the Davos Symposium on Avalanche Formation, Movement and Effects (IAHS Publ. No. 162, 1987), pp. 475 – 508.

Norwegian Geotechnical Institute (1996)

Computational models for dense snow avalanche motion.

NGI report 581250-3.

Perla, R.I. (1980)

Avalanche release, motion, and impact.

In Colbeck, S.C. ed. *“Dynamics of snow and ice masses”*. Academic Press, New York, pp. 397 – 462.

RCP GmbH (1999)

STRUREL – A Structural Reliability Analysis Program System.

RCP GmbH, Munich, Germany.

Rosenblatt, M. (1952)

Remarks on multivariate transformation.

Annals of Math. Stat., Vol. 23, No. 3, pp 470-472.